Clinical applications of virtual, non-contrast head images derived from dual-source, dual-energy cerebrovascular computed tomography angiography

D. Han*, X.J. Xie, L. Wen

Medical Imaging Center, The First Hospital Affiliated Kunming Medical College, Kunming, 650032, China

► *Technical note*

ABSTRACT

Background: This study set out to evaluate the utility of cerebrovascular virtual non-contrast (VNC) scans. **Materials and Methods:** Conventional non-contrast (CNC) and dual-energy computed tomography angiography (DE-CTA) head scans were conducted on 100 subjects, of which 46 were normal, 15 had parenchymal hematomas of the brain, 13 had ischemic infarction, 22 had tumors, and 4 had calcified lesions. VNC images were extracted from the DE-CTA head scans by post-processing. The true (or conventional) and VNC images were compared in terms of the mean CT attenuation value and signal-to-noise ratio (SNR) of the cerebral parenchyma, the image quality, the lesion detection sensitivity, and the radiation exposure level. **Results:** The image qualities of the CNC and VNC scans were (4.95 ± 0.22) points and (3.94 ± 0.24) points (t = 31.18, P < 0.05), the mean CT values for the CNC and VNC images were (34.6 ± 2.44) and (28.6 ± 5.40) HU (t = 10.126, P < 0.05), the SNRs were (9.45 ± 1.26) and (6.87 ± 1.77), and the HU for white matter was (t = 11.859, P<0.05), respectively. The effective radiation doses from the DE-CTA head scans and the conventional non-contrast scans were (8.55 ± 0.57) mSv and (9.41 ± 1.00) mSv, respectively. No significant difference in the lesion detection sensitivities was observed between the CNC and VNC scans, except for tiny calcified lesions, which could not be identified by a VNC scan. **Conclusion:** VNC and contrast-enhanced images could be obtained from DE-CTA head scans and could aid in the diagnosis of cerebral lesions. The radiation dose from the VNC scan was less than that from the CNC scan.

Keywords: *Dual-Source CT, dual-energy, cerebrovascular angiography, virtual non-contrast scan, CT angiography.*

INTRODUCTION

The development of computed tomography (CT) has given rise to both multi-slice spiral CT and radiation dose control, aimed at expanding the applications of CT. Furthermore, the temporal resolution of DE-CT angiography (DE-CTA) head scans has been improved to enable the capture of much clearer images. In addition, the single radiation dose required to obtain virtualnon-contrast (VNC) and contrast-enhanced images has been reduced [1-2]. Nowadays, VNC is widely applied to multiple organs, included the head [3], but is usually applied to hemorrhages and ischemia. In our study, tumors and calcifications were also included to find the accuracy and consistency of VNC and CNC, which would be of great importance to clinics.

MATERIALS AND METHODS

Experimental subjects

Between March 2008 and January 2009, 100 patients were examined by means of DSCT CTA. They consisted of 62 males and 38 females, ranging in age from 18 to 78 (the mean age was 51). Of these, 15 had hematomas, 13 had ischemic infarctions, 22 had tumors, and 4 had calcified lesions. The remainder had no obvious lesions. Exclusions: those who were allergic to the iodine contrast agent, were pregnant, or who had severe heart or kidney dysfunction. This study was conducted with approval from the Ethics Committee of the First Hospital Affiliated Kunming Medical College. Written informed consent was obtained from all participants.

Scanning and post-processing protocol

The CTA scanning and image post-processing are described in table 1. Conventional non-contrast (CNC) scan: True non-contrast scans were performed from the canthomeatal line (CML) to the top of the calvarium.

DE-CTA scan: An injection flow rate of 4 ml/s to 4.5 ml/s was used to give a total injection volume of approximately 60 ml to 70 ml. Bolus tracking was adopted to monitor the concentration of the contrast material within the region of interest (ROI) and to trigger the scanning process. The ROI plane was placed at the bifurcated part of the left common carotid artery, and the threshold was set to 100 HU. Each scan was started 2 s after it was triggered (delay).

Image analysis

One senior attending physician and one postgraduate student analyzed the images independently. A professor was called on to give judgment in any cases of inconsistencies between the analyses.

A five-point scale for grading the image quality was used [4]. The scale ran as follows –5: "excellent," with distinct anatomical details; 4: "good," with the anatomical structures, details, and lesions visible; 3: "fair," with most of the anatomical structures sufficiently clear for diagnosis but some being unsuitable; 2: "poor," with anatomical details that are not clear enough to be distinguishable; 1: "very poor," with only barely recognizable anatomical details that cannot be used for diagnosis. An image quality of > 3 satisfies the basic diagnostic requirement.

For the CNC images, an ROI with an area of 1 cm^2 was identified in the brain stem, and the same ROI in the VNC images was obtained from the true non-contrast images [5]. The signal-to-noise ratio (SNR) was computed as the ratio of the mean CT attenuation value to its standard deviation [6].

Table 1. Head conventional non-contrast and DE-CTA scan parameters.

Scan Parameters	Plain scan	DE-CTA	
		A tube	B tube
KV	120	140	80
mAs	250	51	213
Pitch	0.8	0.7	
Rotate Time (s)	0.5	0.5	
FOV (mm)	210~250	210~250	
Acquisition (mm)	24×1.2	64×0.6	
Kernel Window	H31 medium smooth Cerebrum	H20f smooth CT Angio	
Reconstruction Thickness (mm)	-	1.0	
Reconstruction Increment (mm)	-	0.7	
Thickness (mm)	10	-	
Increment (mm)	10	-	

KV: kilovolt. **mAs:** milliampere second. **FOV:** field of view. **Kernel:** reconstruction algorithm.

Int. J. Radiat. Res., Vol. 14 No. 2, April 2016

160

Radiation dose

CTDI$_{vol}$ represents the average dose for the entire scanning volume, whereas DLP indicates the integrated radiation dose for the entire CT examination, both being generated by the scanner. The effective dose (ED) is the DLP multiplied by a conversion factor, C [7] (in units of mSv), this being 0.023 for head scans [8].

Statistical analysis

The SPSS 11.0 statistical software was used. P values of less than 0.05 were taken to be statistically significant. The data for the mean CT value and the SNR between the CNC and VNC were compared by means of a paired t-test, as were the radiation doses for the CNC and DE-CTA. The image quality was compared by means of a signed-rank test, while the lesion detection was compared with a χ^2 test.

RESULTS

Mean CT attenuation value and SNR

The mean CT attenuation values of the two groups were significantly different. The mean CT attenuation value for a CNC image was 6 HU higher than that of a VNC image. The SNR of the CNC image was higher than that of the VNC image (table 2).

Image quality

The SNRs of the CNC and VNC were significantly different, indicating that the CNC image was better than the VNC image, although both the CNC and VNC images satisfied the diagnosis criteria (table 2 and figure 1.2).

### Lesion detection

The detected lesions from among the 100 cases are listed in table 2. CNC and VNC produced identical diagnoses for lesions that were larger than 5 mm. However, the VNC scan failed to identify one lesion that was smaller than 5 mm (figures 1.3, 1.4). Furthermore, the VNC scan also failed to find calcification.

Comparison of radiation dose

A comparison of the radiation doses for the two groups in terms of the CTDI$_{vol}$, DTP, and ED produced results that were all significantly different. The CTDI$_{vol}$, DTP, and ED values obtained with the DE-CTA VNC head scans were all lower than those for conventional non-contrast scans. The reduced radiation dose of the VNC scan was calculated as follows: Reduced radiation dose for VNC = 2 × radiation dose for conventional non-contrast scan - radiation dose for DE-CTA (table 2).

DISCUSSION

For the DE subtraction technique [9-11], the same ROI was scanned using two different X-ray energy spectra to obtain two sets of images for subtraction. By analyzing the changes in the CT values of different tissues resulting from the use of different X-ray energies, the tissue densities can be distinguished. Using two X-ray sources, DSCT dual-energy imaging subtracts the iodine contrast agent from the contrast-enhanced image to obtain the VNC image [9]. Locations in the two sets of images frequently do not match, however, which limits the use of MSCT [12]. There are at least three advantages to using VNC: 1) Improved stability of examination and image quality; 2) Reduced radiation dose; 3) Lesser demands on patients and technicians.

In this study, each case was examined with a

Table 2. Comparison between CNC and VNC.

scanning approach	Mean CT attenuation values (HU)	SNR	Scoring points	lesions				CTDIvol (mGy)	DLP (mGy×cm)	ED (mSv)
				hematoma	infarction	tumor	calcification			
CNC	34.6±2.44	9.45±1.26	4.95±0.22	15	13	22	4	30.69±0.20	409.33±43.32	**9.41±1.00**
VNC	28.6±5.40	6.87±1.77	3.94±0.24	15	12	22	4	20.62±0.20	371.58±24.97	**8.55±0.57**
t	10.126	11.859	31.18	-	-	-	-	358.23	4.204	**7.47**
P	<0.05	<0.05	<0.05	-	-	-	-	<0.05	<0.05	**<0.05**

161

Int. J. Radiat. Res., Vol. 14 No. 2, April 2016
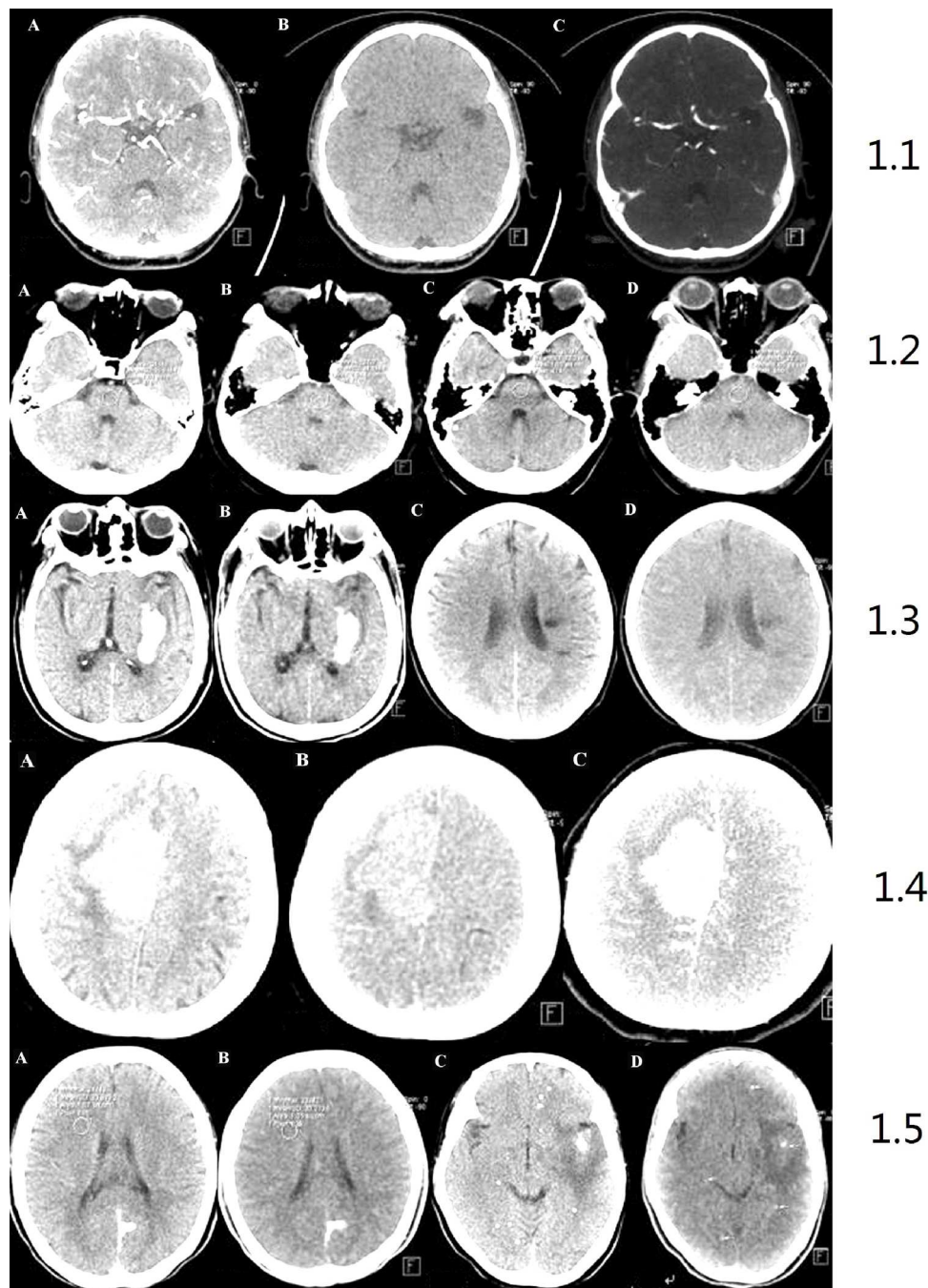
Figure 1. CNC and VNC image of craniocerebral lesion.
1.1: A) merged image; B) VNC image; C) iodine distribution image; 1.2: A) conventional non-contrast scan: 5 points; B) VNC: 5 points; C) conventional non-contrast scan: 4 points; D) VNC: 4 points; 1.3: A) conventional non-contrast scans; B) DE-CTA virtual non-contrast scan Both images show hematoma in left basal ganglia; C) conventional non-contrast scan; D) DE-CTA virtual non-contrast scan.Both images show infarction in left corona radiata area lesion size: 1.4×0.8 cm^2; 1.4: A) conventional non-contrast scan; B) DE-CTA virtual non-contrast scan; C) DE fusion image; the right side parafalx meningioma is demonstrated on all three images; 1.5: A) conventional non-contrast scan; B) DE-CTA virtual non-contrast scanning calcification; in the left occipital lobe is shown on both images; C) conventional non-contrast scan; D) DE-CTA virtual non-contrast scan; multiple calcified lesions are shown on both images, but some tiny calcifications missed on VNC image.

Int. J. Radiat. Res., Vol. 14 No. 2, April 2016

162

conventional non-contrast scan prior to the application of DE-CTA. Although the CNC image was found to be better than the VNC image, the VNC images actually satisfied the diagnostic requirements, while the lesion detection was identical. For lesion diameters of less than 5 mm, as well as tiny calcifications, the VNC method was not as sensitive as CNC.

The radiation exposure for the CT scan was much higher than that for a conventional radiography examination. This would increase the risk of the subject developing cancer [13], while the sub-millimeter sections and small-pitch overlap data acquisition mode in MSCT imaging significantly increases the radiation exposure. The results of this study suggest that DE-CTA is the preferable scanning mode for CTA head scans.

The limitations of this study were related to the small sample size, which may lead to deviations in terms of lesion detection and characterization with a VNC scan. In conclusion, DSCT DE-CTA could not only generate both cerebrovascular contrast-enhanced images and head VNC images through a one-time scan but also reduce the subject's exposure to radiation.

Conflict of Interest: *Declared none.*

REFERENCES

1. Chandarana H, Megibow AJ, Cohen BA, Srinivasan R, Kim D, Leidecker C, Macari M (2011) Iodine quantification with dual-energy CT: phantom study and preliminary experience with renal masses. *AJR Am J Roentgenol,* **196:** W693-700.
2. De Cecco CN, Buffa V, Fedeli S, Vallone A, Ruopoli R, Luzietti M, Miele V, Rengo M, Maurizi Enrici M, Fina P, Laghi A, David V (2010) Preliminary experience with abdominal dual-energy CT (DECT): true versus virtual nonenhanced images of the liver. *Radiol Med,* **115:** 1258-66.
3. Wei H, Yi-ming X, Jin S (2011) Dual-source virtual non-contrast CT of the head: a preliminary study. *Chin J Radiol,* **3:** 229-34.
4. Behrendt FF, Schmidt B, Plumhans C, Keil S, Woodruff SG, Ackermann D, Mühlenbruch G, Flohr T, Günther RW, Mahnken AH (2009) Image fusion in dual energy computed tomography: Effect on contrast enhancement, signal-to-noise ratio and image quality in computed tomography angiography. *Invest Radiol,* **44:** 1-6.
5. Kaufman L, Kramer DM, Crooks LE, Ortendahl DA (1989) Measuring signal-to-noise ratioin MR imaging. *Radiology,* **173:** 265-7.
6. Price RR, Axel L, Morgan T, Newman R, Perman W, Schneiders N, Selikson M, Wood M, Thomas SR (1990) Quality assurance methods and phantoms for magnetic resonance imaging. Report of AAPM Nuclear Magnetic Resonance Task Group No. 1. *Med Phys,* **17:** 287-95.
7. Nakayama Y, Awai K, Funama Y, Liu D, Nakaura T, Tamura Y, Yamashita Y (2006) Lower tube voltage reduces contrast material and radiation doses on 16-MDCT aortography. *AJR Am J Roentgenol,* **187:** W490-7.
8. Menzel H, Schibilla H, Teunen D. European guidelines on quality criteria for computed tomography Luxembourg. European Commission 2000; Publication No. EUR 16262 EN.
9. Johnson TR, Krauss B, Sedlmair M, Grasruck M, Bruder H, Morhard D, Fink C, Weckbach S, Lenhard M, Schmidt B, Flohr T, Reiser MF, Becker CR (2007) Material differentiation by dual energy CT: initial experience. *Eur Radio,* **17:** 1510-7.
10. Scheffel H, Stolzmann P, Frauenfelde T, Schertler T, Desbiolles L, Leschka S, Marincek B, Alkadhi H (2007) Dual-energy contrast-enhanced computed tomography for the detection of urinary stone disease. *Invest Radiol,* **42:** 823-9.
11. Whitman GJ, Niklason LT, Pandit M, Oliver LC, Atkins EH, Kinnard O, Alexander AH, Weiss MK, Sunku K, Schulze ES, Greene RE (2002) Dual-energy digital subtraction chest radiography: technical considerations. *Curr Probl Diagn Radiol,* **31:** 48-62.
12. Lell M, Aanders K, Klotz E, Ditt H, Bautz W, Tomandl BF (2006) Clinical evaluation of bone-substraction CT angiography (BSCTA) in head and neck imaging. *Eur Radiol,* **16:** 889-97.
13. Brenner DJ and Hall EJ (2007) Computed tomography-an increasing source of radiation exposure. *N Engl J Med,* **357:** 2277-84.